A comparative assessment of Power-to-Fuel production pathways

Eleonora Bargiacchi, Marco Antonelli, Umberto Desideri

University of Pisa, Department of Energy, Systems, Territory and Constructions Engineering (DESTEC), Largo Lucio Lazzarino 1, 56122 Pisa (Italy)

Abstract

As the share of intermittent renewable power generation is continuously increasing, energy storage is expected to play a key role in ensuring efficiency, resilience and stability of energy systems. Besides reducing surplus energy curtailments and addressing the issue of seasonal storage, the implementation of some Power-to-X technologies could be an effective supporting tool to decarbonization policies. This paper aims at quantifying Power-to-X process efficiencies and assessing under which conditions they could be carbon neutral during the conversion phase from electricity to a chemical storage, in this case a hydrogen carrier. For this purpose, four synthetic fuel production chains were modelled and simulated with the software Aspen Plus: methane synthesis by means of the Sabatier process, methanol synthesis by carbon dioxide hydrogenation, ammonia production with the Haber-Bosch process and urea synthesis with the Stamicarbon CO_2 stripping process. The production pathways were compared in terms of energy and exergy efficiencies, net CO_2 emissions and specific energy consumption. Emission intensity threshold values for these technologies to be carbon neutral were also estimated. Assuming that the feed hydrogen is produced by electrolysis, the impact of

an upstram electrolyzer upon the aforementioned parameters was assessed and discussed. The produced fuels can subsequently be employed as raw chemicals or as fuels in the mobility or power sectors (the so-called X-to-Power). However, the further processing of the analyzed fuels is not included in the present work.

Keywords: Electrofuels, Hydrogen, Methane, Methanol, Ammonia, Urea, Sabatier reaction, Haber-Bosch, Bosch-Meiser

---

Nomenclature

Abbreviations

C	Compressor
D	Distillation Column
DUFC	Direct Urea Fuel Cell
EI	Emission Intensity
FC	Fuel Cell
GHG	Greenhouse Gases
HE	Heat Exchanger
IC	Intercooler
LHV	Lower Heating Value
PEMFC	Proton Exchange Membrane Fuel Cell
PtG	Power-To-Gas
PtL	Power-To-Liquid
PtX	Power-To-X
R	Reactor
RES	Renewable Energy Sources

SEC	Specific Energy Consumption	
SEP	Separator	
SOFC	Solid Oxide Fuel Cell	
T	Turbine	
Greek letters		
ρ	Density	$[\ \mathrm{kg\,m^{-3}}\ ]$
Latin letters		
$\dot{m}$	Mass flow rate	$[\ \mathrm{kg\,s^{-1}}\ ]$
$\dot{Q}$	Heat flow rate	$[\ \mathrm{J\,s^{-1}}\ ]$
$\dot{W}$	Work flow rate	$[\ \mathrm{J\,s^{-1}}\ ]$
H	Enthalpy	$[\ \mathrm{J\,mol^{-1}}\ ]$
Indices and Exponentials		
comb	Combustion	
el	Electricity	
eq	Equivalent	
nat	Natural	
syn	Syngas	
th	Thermal	

1. Introduction

Industrialization and the extensive use of fossil fuels has produced a significant increase of GHG emissions during the last decades, with 32,294 Mt CO_2 emitted in 2015, which is 48% more than in 1973 [1]. European policies addressing climate issues, in particular the '20-20-20' target, increased RES (Renewable Energy Systems) installation and stimulated a growing interest

in process energy efficiency. The EU average share of renewable energy in 2016 was 29.60%, 7.13%, 19.06% in power generation, transportation and heating and cooling sectors respectively, a huge increase if compared to 2004 (14.30%, 1.39%, 10.26% respectively) [2]. The growing penetration of intermittent sources (namely wind and photovoltaic power plants) causes grid overloads and poses new challenges in the development of a good mix of energy storage technologies. There are several energy storage technologies (i.e: mechanical, thermal, chemical, electrochemical and electrical), with different operating ranges in terms of capacity, power and response time [3, 4, 5, 6, 7]. Mechanical energy storage technologies are the most mature, with a high efficiency. They cover high capacity ranges but have a response and , except pumped hydro, short discharge time. Electrochemical (batteries) and electrical storage systems have very fast response but relatively short discharge times. Chemical energy storage can reach high storage capacities with long response and discharge times. Nowadays, no energy storage technology outperforms the others in all technical characteristics, and the selection of the most suitable technology is case-related, depending on the power generation mix, demand/supply mismatch in terms of power and time, amount of energy to be displaced with time. There is not a single optimal solution for energy storage, but there may be different energy storage technology mixes for grids with different renewable energy mixes. It is nonetheless clear that among the currently available and known energy storage technologies, the conversion of electric into chemical energy by producing a fuel allows the largest storage capacities coupled with the longest discharge times, thus being a very good candidate for daily to seasonal energy storage. In the last decades, hydrogen

has been identified as a feasible and sustainable energy vector. In parallel with the development of better and better fuel cells, the challenges that hydrogen has yet to cope with are its low energy density at ambient conditions and the construction of a widespread distribution network. Power-to-fuels technologies allow to continue using the same infra-structure and know-how of existing technologies in the mobility sector (internal combustion engines) and power generation (natural gas fueled combined heat and power plants). Besides this, the investigated fuels could be employed in low impact emerging technologies such as fuel cells (FCs), which could play a key role in the energy transition both in stationary applications [8, 9] and in the transportation sector [8, 10]. Methane has been successfully tested both in Proton Exchange Membrane (PEMFCs) and in Solide Oxide Fuel Cells (SOFCs) with internal reforming [11, 12, 13]. Direct Methanol Fuel Cells (DMFCs) have been identified as promising, stable and efficient conversion mechanisms, so that they were proposed to power portable devices [14, 15]. Ammonia can be employed in direct ammonia and alkaline membrane fuel cells, direct hydrazine and ammonia borane fuel cells and direct ammonia solid oxide fuel cells [16]. Finally, in recent years urea has been studied for different applications [17, 18] and Direct Urea Fuel Cells (DUFCs) have made significant improvements also when fed with contamined water [19]. Some of the fuels that can be synthesized in PtX (Power-to-X with X meaning a gaseous or a liquid fuel) processes are liquid at environmental conditions, which avoids energy intensive steps to store them at high pressures or low temperatures, and are produced by using carbon dioxide as feed, which makes these technologies supporting means to decarbonization or carbon utilization policies. However,

fuel synthesis by thermochemical processes requires complex and energy intensive production chains, with relatively high costs and lower efficiencies if compared with simpler technologies such as electric and electrochemical storage.

In the last decades, several authors have studied alternative fuels from different points of view: economic impact, life cycle assessment, fuel properties etc. To cite some of them, Schemme et al. [20] wrote a review of renewable fuels that can replace diesel on the basis of their physical, chemical and combustion properties, production costs and technical maturity. Lan et al. [21] focused on hydrogen storage into ammonia and ammonia related chemicals (ammonia borane, ammonia, ammine salts and inorganic ammonium salts) and their usage in fuel cells. Elishav et al. [22] investigated the technical and economic feasibility of nitrogen based fuels as energy carriers, in comparison with batteries, compressed air, pumped hydro and renewable methanol.

In this framework, a few authors ([23], [24], [25], [26]) carried out a comparative study among production chains of fuels from hydrogen and carbon dioxide based on energy and exergy efficiency of conversion technologies.

This paper follows a similar approach and compares four Power-to-Fuel production chains in terms of energy and exergy efficiencies, net CO_2 emissions and specific energy consumption. The investigated technologies are:

- Sabatier process for methane synthesis
- Carbon dioxide hydrogenation for methanol synthesis
- Haber-Bosch process for ammonia synthesis
- Stamicarbon CO_2 stripping process for urea synthesis

We concentrated the attention to the four fuels that we consider the most promising to store significant amount of energy and are based on well known chemicals with commercially assessed processes and storage technologies. According to the authors knowledge no previous paper has been published with such a comparison of different fuel production chains.

2. Selection of fuels and conversion technologies

Most Power-to-Fuel technologies need hydrogen. Most fuels are in fact hydrogen carriers and hydrogen has to be produced from renewable energy to be used in such further conversion processes. Hydrogen produced from fossil fuels would not contribute to fuel decarbonization. Among the various alternative fuels and conversion pathways listed in the literature, the fuels selected for this study, namely, methane, methanol, ammonia and urea (see Table 1 for their most relevant properties), rank among the most promising hydrogen carriers [26, 27] and are produced by well-established and widespread process chains. Since the paper aims at applying existing or emerging technologies to implement Power-to-X (at least in the starting phase), when possible, simulation parameters have been kept as close as possible to benchmark or literature values. While Haber-Bosch and Stamicarbon plant design and operating parameters are quite established and available in literature ([28, 29], [30]), methanol is commercially produced by catalytic conversion of syngas by fossil fuels, therefore its production from CO_2 and H_2 is at an earlier stage. In the present work, a literature plant configuration has been adopted [23]. Among the several commercial methanation concepts [31], a fixed-bed reactor was chosen, operating at an average temperature and pressure in the

ranges reported by literature ([32]).

Table 1: Specifications of the fuels considered in the present study

Fuel	Formula	Molar Mass	ρ[1]	LHV	Energy density	H_2 content
Unit		g/mol	kg/m^3	MJ/kg	GJ/m^3	(wt%)
Methane (v)	CH_4	16.04	0.67 [33]	50.0 [34]	33.53 $\cdot 10^{-3}$ [33]	25.2
Methanol (l)	CH_3OH	32.04	0.796 $\cdot 10^3$ [27],[33]	19.9 [34]	15.58 [35]	12.5
Ammonia (v)	NH_3	17.03	0.719 [33]	18.6 [36],[27]	14.1$\cdot 10^{-3}$ [36]	17.6 [37]
Urea (s)	CH_4N_2O	60.05	1.32 $\cdot 10^3$ [37]	10.5 [35]	13.89 [35]	6.7 [37]

2.1. Methane synthesis pathway

Methane at ambient conditions is a colorless and odourless gas. It is the main component of natural gas, that in 2015 accounted for 21.6% of the world primary energy supply, with a total of more than 3600 billion m^3 [1]. In recent years, studies on how to produce methane from CO_2 and H_2 have grown in number. Methanation can be performed both in catalytic and biological reactors, using the Sabatier methanation process (Eq. 1).

$$4H_2 + CO_2 \rightleftharpoons CH_4 + 2H_2O \quad \Delta H^\circ{}_{298\ \mathrm{K}} = -165kJ/mol \tag{1}$$

The reaction is highly exothermic and thermodynamically favoured at high pressures and low temperatures, which on the other hand slows the kinetics down. In recent years researchers have been focused on achieving stable catalysts at low temperatures [38]. Depending on the process and on the chosen catalyst, the Sabatier reaction operating parameters vary considerably. The

[1] at 15°C, 1 bar

Sabatier reaction is also employed in a plant that was recently put into operation by ETOGAS for AUDI in Wertle (Northern Germany) [39], which proved the technical feasibility of industrial-scale power-to-methane plants.

2.2. Methanol synthesis pathway

Methanol is one of the most important raw materials in chemical industry. Worldwide production capacity in 2015 was around 70 million metric tons (138 billion liters), driven in large part by emerging energy applications, which now account for 40% of the total consumption [40]. Methanol is currently produced at an industrial scale by catalytic conversion of synthesis gas derived from carbonaceous fuels (coal, natural gas, petroleum and its heavy fractions). Among these, natural gas is the most used raw material for synthesis gas production in large-scale methanol synthesis processes. The reaction is operated at high pressures (50-100 bar) and relatively low temperatures (200℃-300℃) [41], on $Cu - ZnO - Al_2O_3$ catalyst. In the last years, however, an increasing number of researches ([42, 43, 44, 45, 46]) have dealt with methanol production from CO_2 and H_2. Although still under development, the technical feasibility of a sustainable methanol production has been proven by the establishment of two pilot demonstration-scale plants by Mitsui Chemicals [47] in Germany and Carbon Recycling International CRI [48] in Iceland.

During methanol synthesis from hydrogen and carbon dioxide, the following main reactions occur:

$$CO_2 + 3H_2 \rightleftharpoons CH_3OH + H_2O \quad \Delta H^\circ{}_{298\ \mathrm{K}} = -49.4 kJ/mol \tag{2}$$

$$CO + 2H_2 \rightleftharpoons CH_3OH \quad \Delta H^\circ{}_{298\ \mathrm{K}} = -90.55 kJ/mol \tag{3}$$

$$CO_2 + H_2 \rightleftharpoons H_2O + CO \quad \Delta H^\circ{}_{298\ \mathrm{K}} = +41.12 kJ/mol \tag{4}$$

2.3. Ammonia synthesis pathway

Because of its numerous applications, ammonia is the second largest synthetic chemical product in the world. Besides its many uses, energy-related applications include its use in fuel cells [16] and in spark ignition engines, eventually in presence of a combustion promoter such as hydrogen [49]. In this paper the Haber-Bosch synthesis plant was considered, since this process covers more than 90% of the current production [41]. It relies on the catalytic reaction of hydrogen and nitrogen according to Eq. 5:

$$N_2 + 3H_2 \rightleftharpoons 2NH_3 \quad \Delta H^\circ{}_{298\ \mathrm{K}} = -92.4 kJ/mol \tag{5}$$

2.4. Urea synthesis pathway

Urea is a non-flammable, relatively non-toxic, colorless, anisotropic cristalline solid. Its stability, non-flammability and high density at environmental conditions make urea a favorable hydrogen carrier substance offering the potential to be easily transported and stored [37]. Urea main applications are soil and leaf fertilization (more than 90% of the total use [41]), formaldehyde resins and melamine production, and, besides other miscellaneous applications, NO_x emission abatement from flue gases of power plants or diesel engines. In recent years, urea has been tested in fuel cell stacks [50, 35, 17, 18, 51], with the efficiency reaching 60% [35]. Industrially, urea is synthetised from ammonia and carbon dioxide by the Bosch-Meiser reaction. The process is based on two reactions: with the first, ammonium carbamate is formed

from ammonia and carbon dioxide (see Eq. 6) in a fast, highly exothermic reaction; with the second, carbamate is decomposed into urea and water in a slow and slightly endothermic reaction (see Eq. 7).

$$2NH_3 + CO_2 \rightleftharpoons H_2N - COONH_4 \quad \Delta H^\circ{}_{298\ \mathrm{K}} = -117kJ/mol \tag{6}$$

$$H_2NCOONH_4 \rightleftharpoons (NH_2)_2CO + H_2O \quad \Delta H^\circ{}_{298\ \mathrm{K}} = +15.5kJ/mol \tag{7}$$

Several industrial processes are used to produce urea, namely KM-CDR, Snamprogetti and Stamicarbon processes. In this study, the Stamicarbon CO_2 stripping process has been analyzed, since it is reported to hold the largest market share [30].

3. Methodology

The investigated processes were modelled with the software Aspen Plus V9. The methods employed for the simulations were the PENG-ROB for the methane, methanol and ammonia synthesis plants, and the SR-POLAR for the urea plant. A unit mass flow rate (1 kmol/s) of hydrogen and a second reactant in stoichiometric ratio were introduced as feeds into each plant.

3.1. Model assumptions

The model main assumptions are the following:

- Process components were assumed to operate without any pressure drop;
- Simulations were performed using steady state chemical reactors and reaction kinetics was not taken into account.

3.2. Efficiency calculations

Pathway energy and exergy efficiencies were calculated through Eq. 8 and 9:

$$\eta_I = \frac{\dot{Energy}_{out}}{\dot{Energy}_{in}} = \frac{\dot{m}_{fuel} \cdot LHV_{fuel}}{\sum_{i=1}^{n} \dot{m}_{syn,in,i} \cdot LHV_{syn,i} + \sum_{j=1}^{m} \dot{Q}_{in,j} + \sum_{k=1}^{q} \dot{W}_{in,k}} \tag{8}$$

$$\eta_{II} = \frac{\dot{Exergy}_{out}}{\dot{Exergy}_{in}} = \frac{\dot{m}_{fuel} \cdot LHV_{fuel}}{\sum_{i=1}^{n} \dot{m}_{syn,in,i} \cdot LHV_{syn,i} + \sum_{j=1}^{m} \dot{Q}_{in,j} \cdot (1 - \frac{T_0}{T_j}) + \sum_{k=1}^{q} \dot{W}_{in,k}} \tag{9}$$

In the term "energy/exergy out" only the energy/exergy content of the product stream was considered; the exploitation of other useful effects (waste heat recovery and regeneration) was not taken into account in this first analysis. Moreover, it has to be noted that expanders duty was not deducted from the compressor total duty to keep the assessment as comprehensive as possible (i.e: the expander electricity could either feed the compressors, or be delivered to the grid). Both of the just mentioned implementations would improve the plants efficiency and will be briefly discussed in section 5.

3.3. Carbon dioxide emissions calculation

The net carbon dioxide emissions were calculated according to Eq. 10.

$$CO_{2,net} = CO_{2product,out} + CO_{2,eq.heat} + CO_{2,eq.el.} - CO_{2feed,in} \tag{10}$$

$CO_{2,eq.el.}$ and $CO_{2,eq.heat}$ represent the equivalent amount of carbon dioxide that is emitted to produce a certain quantity of electricity or heat. $CO_{2,eq.el.}$ is computed from the emission intensity (EI) for the production of unit of

electric energy (Eq. 11). It depends on the energy mix of the country. Emission intensity for european countries can be found in reference [52].

Differently, for the $CO_{2,eq.heat}$ value it is assumed that the heat used in the simulated processes is produced in natural gas industrial boilers. The emission intensity value is therefore divided by the boiler efficiency (η_{comb}=0.9) (see Eq. 12).

$$CO_{2,eq.electricity} = EI_{CO_2,el} \cdot kWh_{el} \tag{11}$$

$$CO_{2,eq.heat} = \frac{EI_{CO_2,nat.gas} \cdot kWh_{th}}{\eta_{comb}} \tag{12}$$

3.4. Impact of the electrolysis process

Assuming that the hydrogen employed as feed in all investigated conversion processes is produced by electrolysis, the aforementioned calculations were repeated by adding an upstream electrolyzer for hydrogen production. In this case, Eq.10 was applied for CO_2 emissions calculation, while energy and exergy efficiencies were calculated according to Eq. 13 and 14:

$$\eta_I = \frac{\dot{Energy}_{out}}{\dot{Energy}_{in}} = \frac{\dot{m}_{fuel} \cdot LHV_{fuel}}{\frac{\sum_{i=1}^{n} \dot{m}_{syn,in,i} \cdot LHV_{syn,i}}{\eta_{electrolysis}} + \sum_{j=1}^{m} \dot{Q}_{in,j} + \sum_{k=1}^{q} \dot{W}_{in,k}} \tag{13}$$

$$\eta_{II} = \frac{\dot{Exergy}_{out}}{\dot{Exergy}_{in}} = \frac{\dot{m}_{fuel} \cdot LHV_{fuel}}{\frac{\sum_{i=1}^{n} \dot{m}_{syn,in,i} \cdot LHV_{syn,i}}{\eta_{electrolysis}} + \sum_{j=1}^{m} \dot{Q}_{in,j} \cdot (1 - \frac{T_0}{T_j}) + \sum_{k=1}^{q} \dot{W}_{in,k}} \tag{14}$$

Even if higher efficiencies for water electrolysis are reported in literature [53], a precautionary value of 0.6 (LHV based) was adopted [54], with a

correspondent specific energy consumption (SEC) of 55.6 kWh/kg H_2, which falls in the normal SEC range for alkaline and PEM electrolyzers [55].

4. Plant layouts and model development

4.1. Methane

The methanation reactor (Fig. 1) is fed with CO_2 and H_2 in stoichiometric ratio (1:4 according to Eq. 1) at ambient conditions (25℃ and 1 bar). The gases are compressed at 60 bar in an intercooled compressor. Reaction is carried out in a Gibbs reactor at 300℃ and 60 bar (Table 2). The products of reaction cool down in a heat exchanger, heating water at around 100℃. Finally, methane is separated from liquid water in a flash separator. The higher the pressure, the more the reaction equilibrium shifts towards the products side. The 60 bar pressure has been chosen to have a high methane purity (≥97% in mass fraction) in the product stream without adding more separators. After being separated from by-products, methane needs to be stored or fed into high-pressure pipelines (50-60 bar).

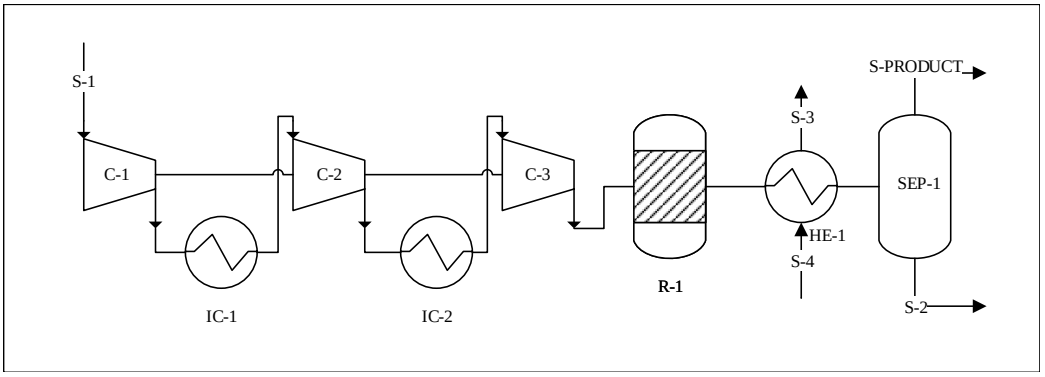

Figure 1: Flowsheet for the methane production plant

Table 2: Process specifications for the methane production plant

Specification	Unit	C-3	R-1	HE-1	SEP-1
Temperature	℃	-	300	-	30
Pressure	bar	60	60	-	60
Hot stream outlet temperature	℃	-	-	30	-

4.2. Methanol

The modeled plant (Fig. 2) is fed with 1 kmol/s of H_2 and a stoichiometric quantity of CO_2 (ratio 3:1) at ambient conditions. The feedstock is then compressed in a multi-stage intercooled compressor up to 50 bar. The reaction occurs at 200℃ and 50 bar in a Gibbs reactor, and the products are then expanded in an isentropic turbine to 20 bar to reach the most suitable separation pressure (Table 3). At lower separation pressure, it is more difficult to separate water from liquid methanol. At downstream pressure higher than 20 bar a smaller electric output would be generated without significant improvements in methanol purity. Primarily, the educts are flashed in a separator: the vapour phase is still rich in hydrogen and carbon dioxide and is partly recycled and mixed with the feedstock; the liquid stream is sent to a distillation column with 20 stages, feed stage in position 17 and partial condenser [23]. Reflux and distillate-to-feed mole ratios have been tuned to obtain a methanol mass fraction higher than 98% in the product stream and lower than 2% in the "water" stream.

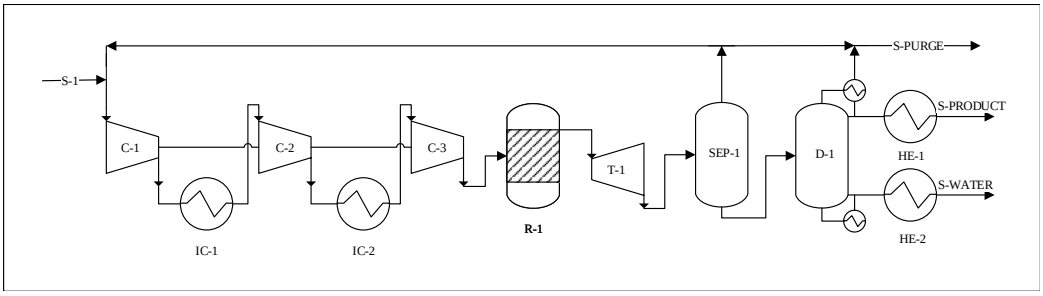

Figure 2: Flowsheet for the methanol production plant [23]

Table 3: Process specifications for the methanol production plant

Specification	Unit	R-1	C-3	T-1	SEP-1	D-1	HE-1	HE-2
Temperature	℃	200	-	-	25	25	25	25
Pressure	bar	50	50	20	20	-	-	-

4.3. Ammonia

Nitrogen and hydrogen are introduced into the plant (Fig. 3) in stoichiometric ratio (1:3), at ambient conditions. After being adiabatically mixed with the recycled vapour stream coming from the second separator, they are compressed by a three-stage intercooled compressor with a final discharge pressure of 250 bar. Reactants are pre-cooled by exchanging heat with the cold gases, ammonia-rich stream coming from the expander and then subjected to a first flash separation (SEP-1) at 0℃ (Table 4). The vapour stream in SEP-1 is rich in unreacted hydrogen and nitrogen and is partly recycled towards HE-2; the liquid stream from SEP-1 is mixed with the liquid one from SEP-2, both rich with ammonia, and is further flashed in a vapour-liquid flash separator (EXP-1). Its purpose is to split the ammonia-rich educt and further purify it into a liquid stream (ammonia purity grade $\approx$ 99.9%) and

a vapour stream containing some unreacted components. After being mixed with a portion of the liquid stream, the gaseous ammonia (purity$\geq$98%) is heated in a counter-current heat exchanger by the hot reactants coming from the inter-cooled compressor into HE-1. The vapour obtained by flash separation in the block SEP-1, mainly composed of hydrogen and nitrogen, is split into two streams, one to be purged and one that is first pre-heated in block HE-2 and then compressed in a single stage compressor up to the reactor operating parameters (400℃ and 200 bar). The gaseous products are used to pre-heat the reactants in block HE-2 and finally flashed in a flash separator (SEP-2).

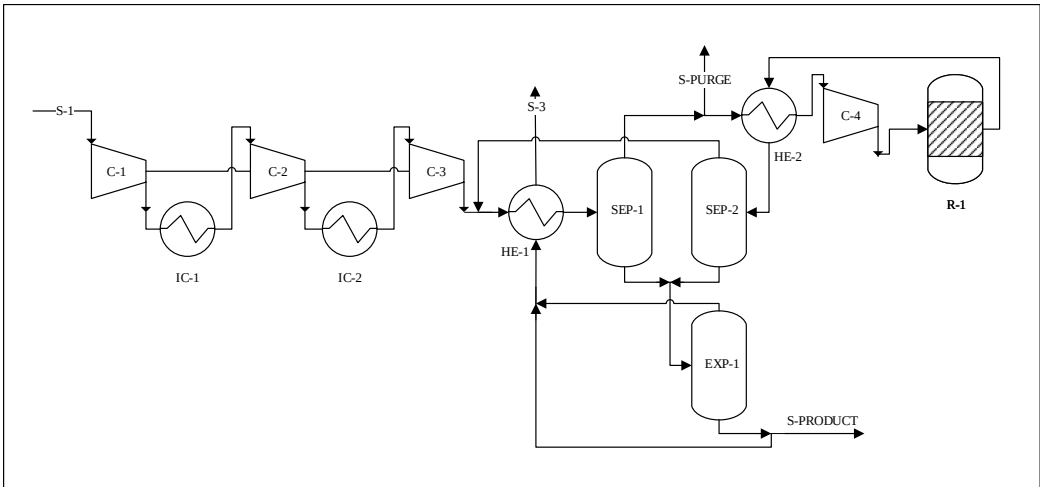

Figure 3: Flowsheet for the ammonia production plant [29]

4.4. Urea

As for the previous fuels, the reactants NH_3 and CO_2 are fed to the plant (Fig. 4) in stoichiometric ratio 2:1. Compressed carbon dioxide feeds

Table 4: Process specifications for the ammonia production plant

Specification	Unit	C-3	HE-1	SEP-1	SEP-2	R-1	EXP-1
Temperature	℃	-	0	25	400	-	-
Pressure	bar	250	-	250	250	250	1
Outlet vapour fraction		-	1	-	-	-	-
Duty	kW	-	-	-	-	-	0

the high-pressure stripper (E-1), where carbamate-rich urea solution coming from the reactor is thermally decomposed into NH_3 and CO_2 by heat and the CO_2 flow itself. The liquid stream, rich in urea, is sent to a second reactor (R-2) and a separator (SEP-3) to be purified. The gaseous effluents from the stripper, mainly carbon dioxide and urea, plus ammonia and the liquid stream from the scrubber are condensed into a high-pressure condenser (E-3), where ammonium carbamate is formed. The urea reactor is simulated as a RPlug adiabatic reactor. Urea solution is synthesized and separated from unreacted gases into a flash separator (SEP-3). The latter are absorbed into the recycled carbamate solution from the low-pressure section, and then mixed upstream with NH_3 and urea solution from E-1.

Ammonia is assumed to be produced by the Haber-Bosch process, which was already explained in section 4.3. The resulting complete urea synthesis process is shown in Fig. 5. In this case the simulation was run with the SR-POLAR method.

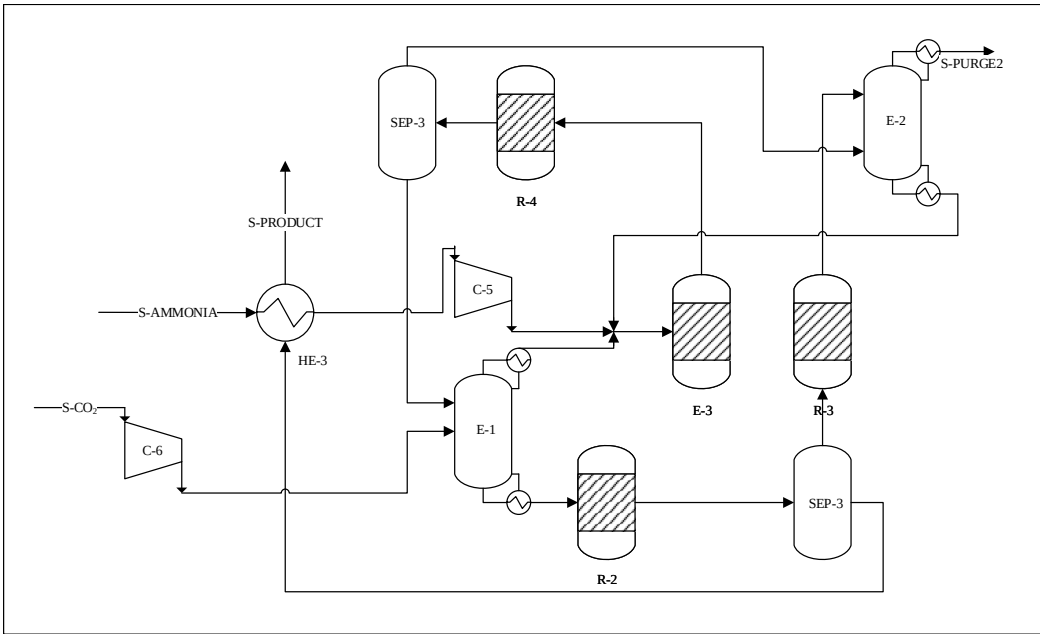

Figure 4: Flowsheet for the urea production plant by Stamicarbon CO_2 stripping process

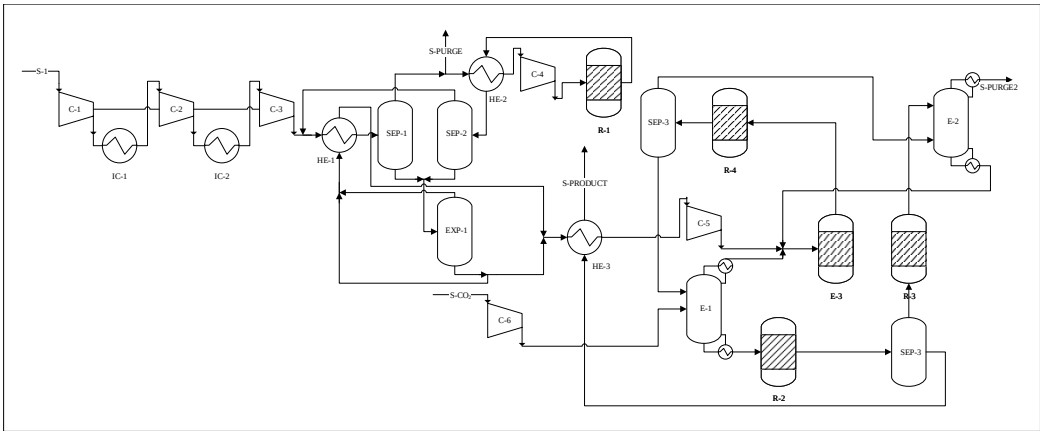

Figure 5: Complete flowsheet for the urea production plant by combining Haber-Bosch and Stamicarbon CO_2 stripping processes

Table 5: Process specifications for the urea production plant (only Bosch-Meiser section)

Specification	Unit	C-6	E-1	HE-3	C-5	E-3	R-4	SEP-3	R-2	SEP-3	R-3	E-2
Temperature	℃	-	-	-	-	167	-	-	72.4	72.4	72.4	-
Pressure	bar	138.3	138.3	-	156.9	138.3	138.3	138.3	138.3	138.3	138.3	138.3
Hot stream outlet temperature	℃	-	-	25	-	-	-	-	-	-	-	-
Duty	kW	-	-	-	-	-	-	0	-	-	-	-

5. Results and discussion

In this section, the simulation results will be illustrated and commented in terms of the parameters described in section 3: energy and exergy efficiencies, specific energy consumption, net CO_2 emissions. First, each process will be analyzed using the Sankey exergy diagrams, then a comparison among all of them will be carried out. It is to be noted that the product exergy value in Sankey diagrams differs slightly from the efficiency since Sankey diagrams also show the material flows physical exergy, which is not taken into account in the efficiency calculation not being a useful effect.

5.1. Exergy balances

5.1.1. Methane

The exergy Sankey diagram (Fig. 6) of the methane production plant shows that the major contribution to the inlet exergy stream is given by the hydrogen chemical exergy (88.4%). The remaining inlet (11.6%) is represented by the compressor electric duty. The largest share (69.7%) of the total exergy is transferred to the products. The reactor outlet stream enthalpy is recovered to produce hot water (T=101℃, p=1 bar), which accounts for 14.6% of the total exergy output and can be re-used inside the plant itself for industrial or sanitary purposes. Being the Sabatier reaction exothermic,

the reactor needs to be continuously cooled, and the exergy of this process is 7.4% of the total outlet. The cooling duty required for the compressor inter-cooling is not negligible (3.8%), with quite high exergy content, since it is discharged at elevated temperature ($\sim$ 300 ℃). The mass fraction of the liquid stream coming from the flash separator contains more than 99.9% water and has a negligible exergy due to its low discharge temperature (30℃). Irreversibilities amount to 4.5% and can be attributed to high-temperature heat transfer inside the plant components.

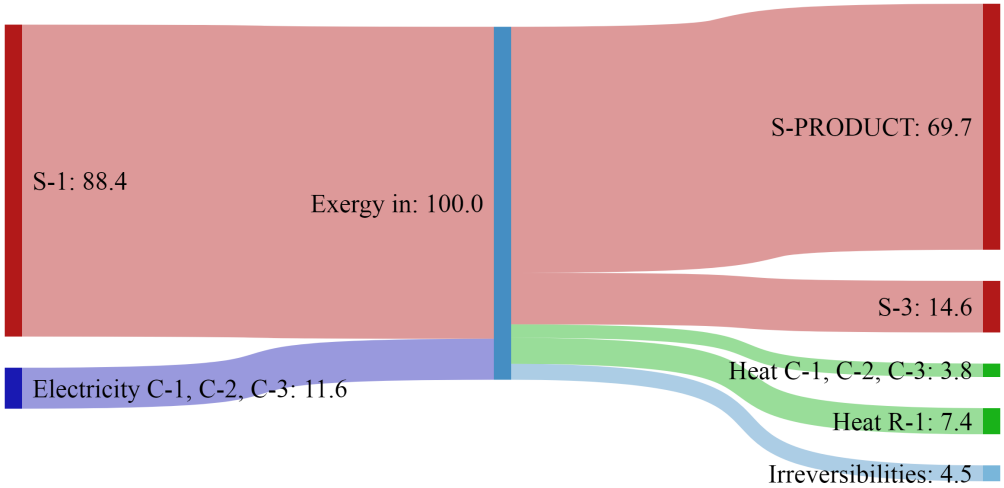

Figure 6: Exergy Sankey diagram for the methane production plant

5.1.2. Methanol

The methanol plant major exergy input is represented by the chemical exergy of the reactants (70.2%) (Fig. 7). Other inputs are the electric energy required by the inter-cooled compressor (29.0%) and the heat duty required by the distillation column (0.8%). The largest exergy share (41.4%) of the total input is stored into the product stream. Compressor inter-cooling duty

is 10.9% of the total exergy input, since heat is discharged at 235℃. The expander produces 5.5 MW of electricity, which can be supplied to the grid or used for the compressor. The heat exchangers HE-1 and HE-2 cool the product streams and release heat to the environment at very low temperature (∼50℃), so they are hardly re-usable and their exergy value is negligible. The purged gas consists of 86% CO_2, 13% H_2, approximately 1% CH_3OH (all as mass fractions) and traces of water vapour, with a resulting lower heating value of 15.45 MJ/kg, and is discharged at 20 bar. Its exergy content is approximately 4.9% of the total. The liquid stream coming from the distillation column still contains methanol (around 27% as mass fraction) which could be recirculated or submitted to further treatment. For this reason, it accounts for a big share of the exergy balance (10.8%). The reactor inter-cooling absorbs 2.2% of the total input. Overall irreversibilities are significant (28.0%) and mainly located in the distillation column, in the compressor inter-cooler and in the heat exchangers.

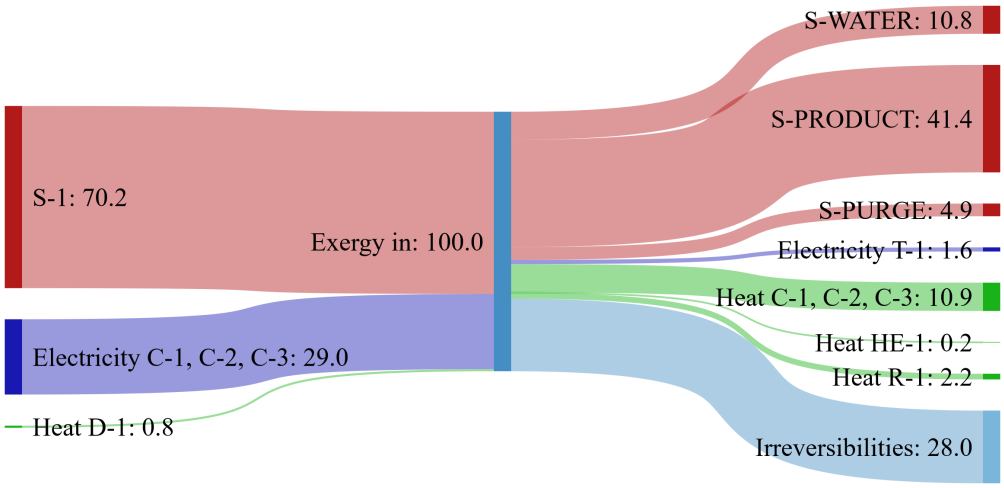

Figure 7: Exergy Sankey diagram for the methanol production plant

5.1.3. Ammonia

In the ammonia production plant the reactants chemical exergy and the compressor duty are the only inputs, which amounts to 86.2% and 13.8% respectively (Fig. 8). The products hold the highest exergy percentage of the total input (52.3%). A considerable exergy amount (28.6%) is contained in the purge stream, which is composed by 78.1% N_2, 16.9% H_2 and 4.9% NH_3 (all in mass fractions), with a resulting LHV of 21.23 MJ/kg. The compressor cooling duty represents 2.7 % of the system exergy output since the heat is released from the stages at relatively low temperatures (i.e: 70℃, 110℃, 150℃). The reactor inter-cooling employs 2.0% of the total exergy input. On the contrary, the heat released by the two flash separators is only 0.1% of the overall exergy output, since the separators operating temperatures are close to ambient. Plant irreversibilities are significant (14.3%) and mainly due to the heat exchangers.

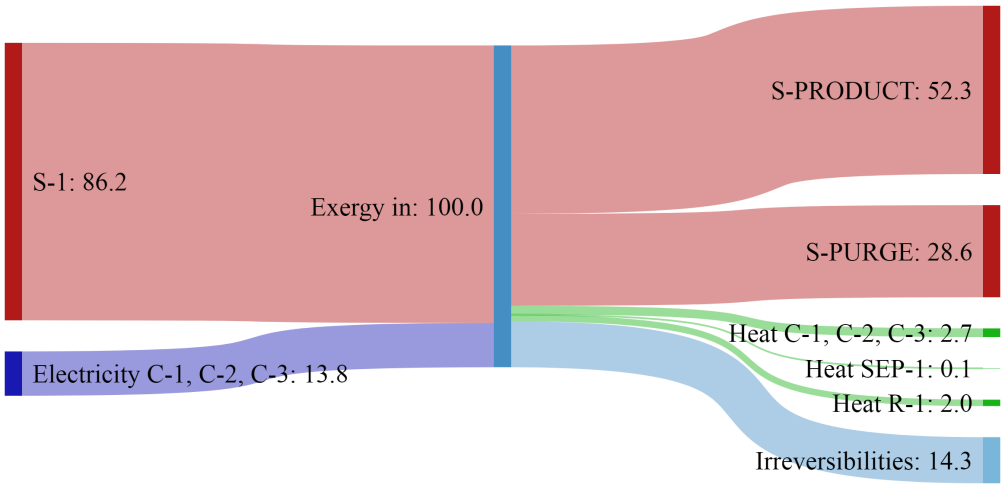

Figure 8: Exergy Sankey diagram for the ammonia production plant

5.1.4. Urea

In the urea production plant, the exergy flows due to the inter-cooled compressor (C-1, C-2, C-3), the reactor (R-1) cooling duty, the flash separators heats (SEP-1 and SEP-2) and the first gas purge (S-PURGE) are the same as in the ammonia plant, and are described extensively in section 5.1.3 (Fig. 9). The flash separator contributions are not present in the diagram since they are negligible. 12.8% of the total exergy input is supplied to the compressors C-5 and C-6 in the Bosch-Meiser process. The last input is the heat supplied to the HP scrubber (E-2), which accounts for 0.4% of the total exergy and is supplied to the unit at relatively high temperature (∼160℃). The purge released to the atmosphere in the Bosch-Meiser section is composed of 83.8% CO_2, 15.5% NH_3 and traces of H_2, N_2, urea and water vapour, giving an average LHV of 2.92 MJ/kg. Since it is purged at 163℃ and 138 bar, it represents the biggest share (47.5%) of the exergy output, for

its high enthalpy and its significant chemical content. The product flows contain only 2.3% of the total entering exergy. Irreversibilities are high (16.2%) and located in the reactors needed to complete the synthesis.

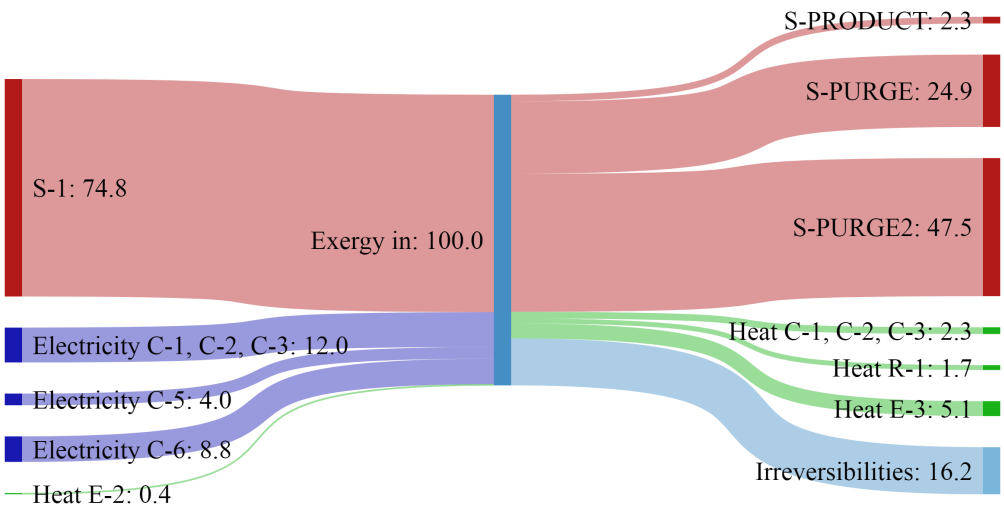

Figure 9: Exergy Sankey diagram for the urea production plant

5.2. Comparison among production pathways

5.2.1. Energy and exergy efficiencies

In Fig. 10 and 11 the energy and exergy efficiencies of the modelled pathways are illustrated. If looking only at fuel production processes, methane synthesis is the most efficient and the one that causes the lowest energy degradation (η_I=η_{II}=72.1%). The second most efficient is the Haber-Bosch process (η_I=η_{II}=51.9%), followed by methanol synthesis (η_I=39.5%, η_{II}=42.1%). As it was predictable, urea is the least efficient for its long chain and the number of energy intensive steps required for the synthesis (η_I=η_{II}=2.3%).

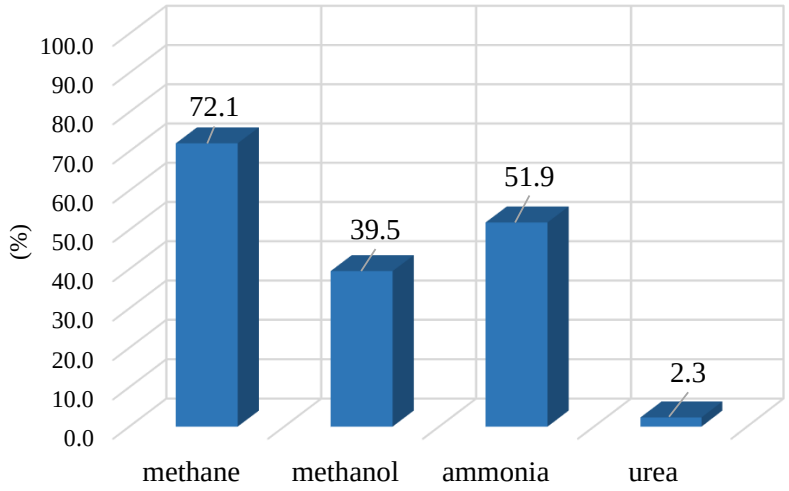

Figure 10: Energy efficiency of the analyzed plants [%]

5.2.2. Waste heat assessment

As complementary byproducts to the fuels, each production chain releases a significant amount of heat and, in some cases, electricity (e.g. electricity produced by the expander in the methanol synthesis plant, if not employed to power the plant compressors). As far as the waste heat is concerned, Fig. 12 shows the plants waste heat as a function of the release temperature, which has been assumed equal to the component operating temperature in the case of reactors, separators and distillation columns, equal to the average heat transfer temperature in the case of heat exchangers and inter-cooled compressors, and equal to the stream temperature in the case of purges. The

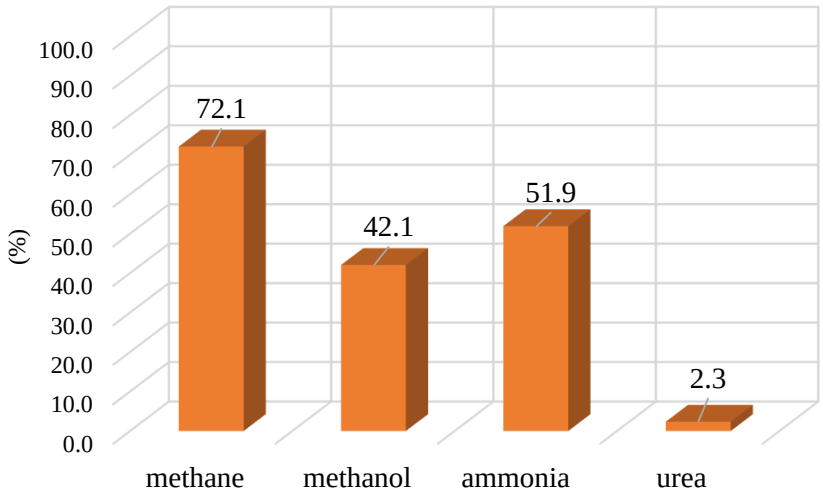

Figure 11: Exergy efficiency of the analyzed plants [%]

components that release heat at ambient temperature are not reported in Fig. 12, since they cannot be further exploited. In methane production plants, the Sabatier reaction releases approximately 45 MW at a temperature of 300℃, while the flue gas cooling and the compressor inter-cooling take place at around 160℃. In the methanol synthesis plant, the largest amount of waste heat is discharged during the feed inter-cooled compression (around 90 MW at 191℃), while the exothermic carbon dioxide hydrogenation releases approximately 20 MW at 200℃ to the environment. The two exchangers duties for the methanol and water cooling are respectively 9.4 MW and 1.7

MW at low average temperatures (44℃ and 54℃). The Haber-Bosch process counts 34 MW at 88℃ for the compressor inter-cooling, 10 MW at 400℃ as reaction heat, which is the only waste heat in the ammonia production process, if we disregard the separators. As far as the waste heat in the Stamicarbon process is concerned, other contributions must be added to the Haber-Bosch waste heat: E-3 releases 51 MW at 167℃, R-2 and R-3 0.76 MW at 72℃ and the plant purge is discharged at 163C, for 2.4 MW of recoverable waste heat in case the flue gases are cooled to 25℃. Most of these heat flows could be fruitfully employed directly to reduce the plant thermal consumption (e.g.: regeneration, pre-heating) or for electricity production (in the case of high temperature flows). From this viewpoint, PtF plants could be intended as polygenerative. The implementation of a waste heat management strategy in all the investigated pathways goes beyond the goal of this work, but it could be a subject of future research.

5.2.3. Electrical, thermal and chemical specific consumption

In Fig. 13 the electrical, thermal and chemical specific consumptions are reported. Among the investigated processes, ammonia has the lowest electric, thermal and chemical energy consumption per kilogram of fuel produced (1.39, 0.00 and 8.67 kWh/kg, respectively). Urea synthesis is the most energy-consuming process. Specific consumption values are listed in table 6.

5.2.4. Decarbonization potential

The plant CO_2 balance is influenced by the carbon emission intensity for electricity, so, ultimately, from the energy mix of the country where the plant

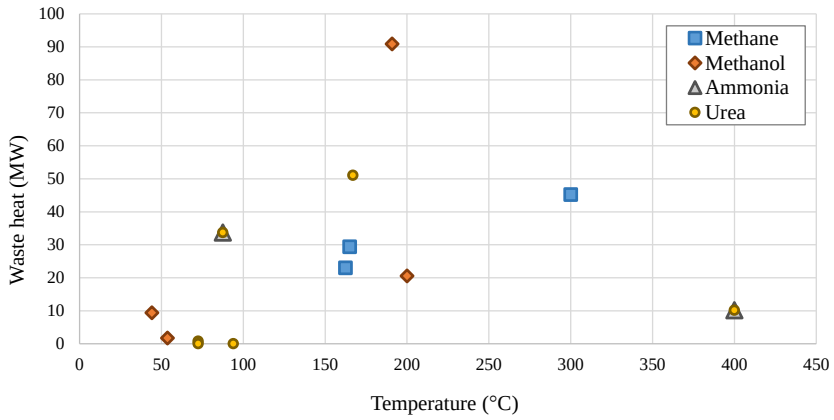

Figure 12: Reusable waste heat as a function of release temperature

is located. In the assumption of being equal to the emission intensity of natural gas combustion, the emission intensity for heat production is not country-dependent. As far as CO_2 emissions are concerned, the values reported in Table 6 are for the Italian case, with a CO_2 intensity for electricity production of 229.2 g/kWh [52]. In the calculation, the emission intensity for natural gas combustion (206.08 g/kWh [56]) has been divided by the average efficiency of industrial boilers (0.9), as explained in section 3. Within the boundaries of the study, namely H_2 and CO_2/N_2 conversion into other chemicals, with the current electricity emission intensities in Italy and Europe (namely, 229.2 g/kWh and 275.9 g/kWh), methane and methanol synthesis plants are car-

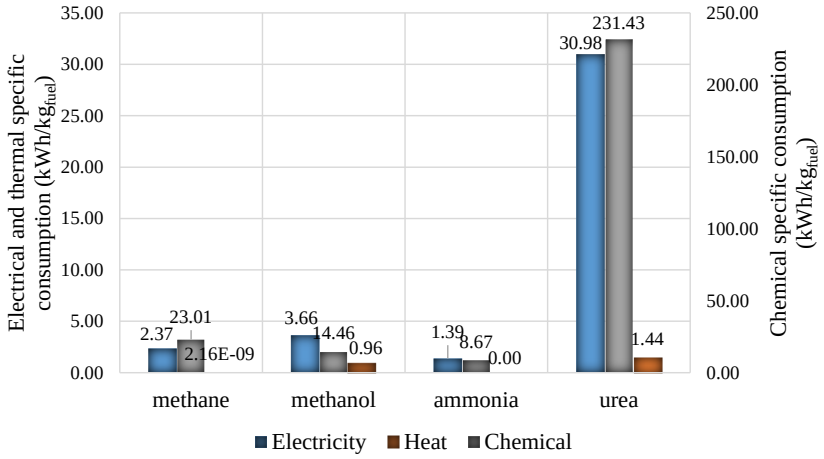

Figure 13: Electric, thermal, chemical specific consumption of the analyzed plants $[kWh/kg_{fuel}]$

bon negative technologies, being able to absorb 2.20 kg_{CO_2}/kg_{fuel} and 2.09 kg_{CO_2}/kg_{fuel}, respectively (see Fig. 14). On the contrary, ammonia and urea production pathways are net carbon emitting sources, producing respectively 0.32 kg_{CO_2}/kg_{fuel} and 6.68 kg_{CO_2}/kg_{fuel} (Italian electricity mix) and 0.38 kg_{CO_2}/kg_{fuel} and 8.12 kg_{CO_2}/kg_{fuel} (average European electricity mix) (see Fig. 14). In the context of an increasing penetration of renewable energy systems in the worldwide energy mix, PtF pathways could potentially be effective technologies for decarbonization. Electricity emission intensities of 1156.0 g_{CO_2}/kWh, 335.0 g_{CO_2}/kWh, 0.0 g_{CO_2}/kWh and 13.7 g_{CO_2}/kWh

are the threshold values below which methane, methanol, ammonia and urea synthesis plants are carbon negative (see Table 6). In other words, any country with an energy mix such as to guarantee an electricity emission intensity lower than the aforementioned values could employ PtF technologies as a path for energy sector decarbonization.

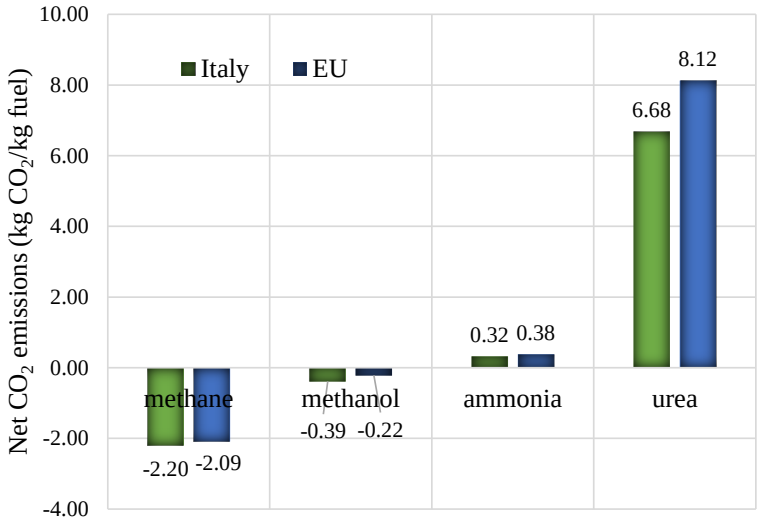

Figure 14: Net carbon emissions of the analyzed plants $[kg_{CO_2}/kg_{fuel}]$

All the aforementioned results for energy and exergy efficiencies, specific consumptions, net carbon dioxide emissions and EI threshold values are displayed in Table 6.

Table 6: Energy and exergy efficiencies and electric, thermal and chemical specific consumptions and net CO_2 emissions for the four investigated fuel production pathways

Fuel	η_I %	η_{II} %	SC_{el} $\frac{kWh_{el}}{kg_{fuel}}$	SC_{th} $\frac{kWh_{th}}{kg_{fuel}}$	SC_{ch} $\frac{kWh_{ch}}{kg_{fuel}}$	Net CO_2 emissions $\frac{kg_{CO_2}}{kg_{fuel}}$	$EI_{el.,thr.}$ $\frac{g_{CO_2}}{kWh}$
Methane	72.1	72.1	2.37	$2.16 \cdot 10^{-9}$	23.01	-2.20	1156.0
Methanol	39.5	42.1	3.66	0.96	14.46	-0.39	335.0
Ammonia	51.9	51.9	1.39	0.00	8.67	0.32	0.0
Urea	2.3	2.3	30.98	1.44	231.43	6.68	13.7

5.3. Impact of the electrolysis process

For the sake of completeness, the different production pathways have been coupled with an upstream electrolyzer for hydrogen production, and the results obtained with the calculations explained in section 3.3 are reported in Table 7. It can be noted that the electrolyzer has a strong impact on the overall process, causing a drop of 26.6%, 11.6%, 18.9% and 0.7% in methane, methanol, ammonia and urea production process energy efficiency, respectively. An electrolyzer efficiency of 0.7 (LHV based) would imply efficiencies of 52.4%, 30.7%, 37.9% and 1.8%, namely, value that is already reported as state of the art by some authors [53]. Net CO_2 emissions with the actual Italian EI for electricity production amount to 4.26 kg_{CO_2}/kg_{fuel}, 3.20 kg_{CO_2}/kg_{fuel}, 3.63 kg_{CO_2}/kg_{fuel} and 42.31 kg_{CO_2}/kg_{fuel} for methane, methanol, ammonia and urea production respectively (see Table 7). The overall processes can be carbon neutral for EI lower than 89.8 g_{CO_2}/kWh, 63.6 g_{CO_2}/kWh, 0.0 g_{CO_2}/kWh, 2.3 g_{CO_2}/kWh for electricity production.

Table 7: Energy and exergy efficiencies and electric, thermal and chemical specific consumptions and net CO_2 emissions for the four investigated fuel production pathways, including upstream electrolysis

Fuel	η_I %	η_{II} %	SC_{el} $\frac{kWh_{el}}{kg_{fuel}}$	SC_{th} $\frac{kWh_{th}}{kg_{fuel}}$	Net CO_2 emissions $\frac{kg_{CO_2}}{kg_{fuel}}$	$EI_{el.,thr.}$ $\frac{g_{CO_2}}{kWh}$
Methane	45.5	45.5	30.54	$2.16 \cdot 10^{-9}$	4.26	89.8
Methanol	27.3	28.5	19.29	0.96	3.20	63.6
Ammonia	33.0	33.0	15.84	0.00	3.63	0.0
Urea	1.6	1.6	186.44	1.44	42.31	2.3

6. Conclusions

In the present work four hydrogen conversion pathways for the production of other easily stockable energy vectors (methane, methanol, ammonia, urea) were modelled with the software Aspen Plus V9. For each, energy and exergy balances were calculated and exergy Sankey diagrams were drawn. They were compared in terms of energy and exergy efficiencies and net carbon emissions to assess and quantify their potential of supporting decarbonization, efficiency improvements in the energy sector and capability to store electric energy from renewable sources. The boundaries of the study included the conversion process from hydrogen and carbon dioxide or nitrogen to a chemical vector, and did not include the X-to-Power reconversion pathway. Accordingly, net carbon reductions have to be intended not referred to the fuel full life-cycle, rather to the aforementioned conversion step. With the analyzed plant layouts, methane production with the Sabatier process is the

most efficient (η_I=η_{II}=72.1%), due to its short production chain. It allows a net carbon emissions reduction of -2.20 kg_{CO_2}/kg_{fuel} and -2.09 kg_{CO_2}/kg_{fuel} with the current Italian and EU emission intensity values for electricity production. The threshold emission intensity value for its being carbon neutral is 1156.0 g_{CO_2}/kWh, that is higher than the actual emission intensities of European countries [52]. The second most efficient technology is the Haber-Bosch process for ammonia production, with energy and exergy efficiencies of η_I=η_{II}=51.9%. Among the investigated plants, it is the process with the lowest electric, thermal and chemical specific consumption (1.39, 0.0 and 8.67 kWh/kg_{fuel}). As the main disadvantage, it has net CO_2 emissions of 0.32 kg_{CO_2}/kg_{fuel} (in the case of the Italian energy mix) and can become a carbon neutral fuel only in case of a substantial redefinition of the country energy mix, since it does not have CO_2 as feed. Methanol synthesis has efficiencies of η_I=39.5% and η_{II}=42.1% and relatively low specific consumption. It is carbon neutral from a threshold value of 335.0 g_{CO_2}/kWh of electric emission intensity, which is higher than the average IE of European Union. Urea is the most energy intensive technology (η_I=η_{II}=2.3%), with high specific energy consumption and relevant net carbon emissions (6.68 kg_{CO_2}/kg_{fuel}) with the current energy mix. Assuming an hydrogen production by electrolysis, the latter severely affects the overall pathway efficiency (up to 27% with an electrolyzer efficiency of 0.6, up to 20% with an electrolyzer efficiency of 0.7). Moreover, since the processes that are investigated in this work are carried out at high temperatures, it is possible to think of an appropriate waste heat management to maximize their efficiency or to use them for polygeneration, which could be the subject of further research. For this reason, the waste

heat flows that could be fruitfully employed instead of being released to the environment were quantified.

Appendix A.

Table A.8: Simulation results for the methane production flowsheet

Specification	Unit	S-1	S-4	S-3	S-2	S-PRODUCT
Temperature	℃	25	25	101.54	30	30
Pressure	bar	1	1	1	60	60
Mass vapour fraction		1	0	0.55	0	1
Mass liquid fraction		0	1	0.45	1	0
Mass flows	kg/s					
CO_2	kg/s	11.00	0	0	0	0.10
H_2	kg/s	2.02	0	0	0	0.02
H_2O	kg/s	0	18.02	18.02	8.93	0.01
CO	kg/s	0	0	0	0	$3.12 \cdot 10^{-5}$
CH_4	kg/s	0	0	0	0	3.98
Mass fractions						
CO_2		0.85	0	0	0	0.02
H_2		0.15	0	0	0	$4.24 \cdot 10^{-3}$
H_2O		0	1	1	1	$1.29 \cdot 10^{-3}$
CO		0	0	0	0	$7.61 \cdot 10^{-6}$
CH_4		0	0	0	0	0.97

Table A.9: Simulation results for the methanol production flowsheet

Specification	Unit	S-1	S-PURGE	S-PRODUCT	S-WATER
Temperature	℃	25	25	25	25
Pressure	bar	1	20	1	1
Mass vapour fraction		1	1	0.01	0
Mass liquid fraction		0	0	0.99	1
Mass flows	kg/s				
H_2	kg/s	2.02	0.30	$1.41 \cdot 10^{-4}$	0
CO_2	kg/s	14.67	2.07	0.14	$2.21 \cdot 10^{-15}$
H_2O	kg/s	0	$3.48 \cdot 10^{-3}$	$7.52 \cdot 10^{-5}$	5.10
CH_3OH	kg/s	0	0.03	7.18	1.86
Mass fractions					
H_2		0.12	0.13	$1.93 \cdot 10^{-5}$	0
CO_2		0.88	0.86	0.02	$3.18 \cdot 10^{-16}$
H_2O		0	$1.14 \cdot 10^{-3}$	$1.03 \cdot 10^{-5}$	0.73
CH_3OH		0	0.01	0.98	0.27

Table A.10: Simulation results for the ammonia production flowsheet

Specification	Unit	S-1	S-PURGE	S-PRODUCT,GAS	S-PRODUCT,LIQ
Temperature	℃	25	0	-33.88	-34.91
Pressure	bar	1	250	1	1
Mass vapour fraction		1	1	1	0
Mass liquid fraction		0	0	0	1
Mass flows	kg/s				
H_2	kg/s	2.02	0.60	0.01	$5.50 \cdot 10^{-7}$
N_2	kg/s	9.34	2.75	0.07	$3.78 \cdot 10^{-6}$
NH_3	kg/s	0	0.17	4.73	3.02
Mass fractions					
H_2		0.18	0.17	$2.61 \cdot 10^{-3}$	$1.82 \cdot 10^{-7}$
N_2		0.82	0.78	0.01	$1.25 \cdot 10^{-6}$
NH_3		0	0.05	0.98	0.99

Table A.11: Simulation results for the urea production flowsheet

Specification	Unit	S-1	S-CO_2	S-PURGE	S-PURGE2	S-PRODUCT
Temperature	℃	25	25	0	163.67	25
Pressure	bar	1	1	250	138.27	138.27
Mass vapour fraction		1	1	1	1	0
Mass liquid fraction		0	0	0	0	1
Mass flows	kg/s					
CH_4N_2O	kg/s	0	0	0	0.01	0.46
$CH_6N_2O_2$	kg/s	0	0	0	$5.08 \cdot 10^{-3}$	0
CO_2	kg/s	0	26.23	0	25.88	0
NH_3	kg/s	0	0	0.26	4.80	0
H_2O	kg/s	0	0	0	0.14	0
N_2	kg/s	9.34	0	4.88	0.07	0
H_2	kg/s	2.02	0	1.06	$8.70 \cdot 10^{-3}$	0
Mass fractions						
CH_4N_2O		0	0	0	$3.38 \cdot 10^{-4}$	1
$CH_6N_2O_2$		0	0	0	$1.64 \cdot 10^{-4}$	0
CO_2		0	1	0	0.84	0
NH_3		0	0	0.04	0.16	0
H_2O		0	0	0	$4.61 \cdot 10^{-3}$	0
N_2		0.82	0	0.79	$2.34 \cdot 10^{-3}$	0
H_2		0.18	0	0.17	$2.81 \cdot 10^{-4}$	0

References

[1] Key World Energy Statistics 2017, Technical Report, Internation Energy Agency IEA, 2017.

[2] Eurostat, Shares tool 2016, http://ec.europa.eu/eurostat/web/energy/data/shares, 2016.

[3] M. Aneke, M. Wang, Energy storage technologies and real life applications A state of the art review, Applied Energy 179 (2016) 350–377.

[4] O. Palizban, K. Kauhaniemi, Energy storage systems in modern gridsâMatrix of technologies and applications, Journal of Energy Storage 6 (2016) 248–259.

[5] B. Zakeri, S. Syri, Electrical energy storage systems: A comparative life cycle cost analysis, Renewable and Sustainable Energy Reviews 42 (2015) 569–596.

[6] M. S. Guney, Y. Tepe, Classification and assessment of energy storage systems, Renewable and Sustainable Energy Reviews 75 (2017) 1187–1197.

[7] A. Gallo, J. Simões-Moreira, H. Costa, M. Santos, E. Moutinho dos Santos, Energy storage in the energy transition context: A technology review, Renewable and Sustainable Energy Reviews 65 (2016) 800–822.

[8] B. C. Ong, S. K. Kamarudin, S. Basri, Direct liquid fuel cells : A review, International Journal of Hydrogen Energy 42 (2017) 10142–10157.

[9] A. Arsalis, A comprehensive review of fuel cell-based micro-combined-heat-and-power systems, Renewable and Sustainable Energy Reviews 105 (2019) 391–414.

[10] L. V. Biert, M. Godjevac, K. Visser, P. V. Aravind, A review of fuel cell systems for maritime applications, Journal of Power Sources 327 (2016) 345–364.

[11] B. Suleiman, A. S. Abdulkareem, U. Musa, I. A. Mohammed, M. A. Olutoye, Y. I. Abdullahi, Thermo-economic analysis of proton exchange membrane fuel cell fuelled with methanol and methane, Energy Conversion and Management 117 (2016) 228–240.

[12] J.-e. Hong, B. Jord, R. Steinberger-wilckens, P. Em, Ceria-Co-Cu-based SOFC anode for direct utilisation of methane or ethanol as fuels (2019).

[13] J. Goo, O. Sung, H. Jung, J. Jang, Y. Lee, S. Hoon, Y. Gun, Durable and High-Performance Direct-Methane Fuel Cells with Coke-Tolerant Ceria-Coated Ni Catalysts at Reduced Temperatures, Electrochimica Acta 191 (2016) 677–686.

[14] S. Kamarudin, F. Achmad, W. Daud, Overview on the application of direct methanol fuel cell (DMFC) for portable electronic devices, International Journal of Hydrogen Energy 34 (2009) 6902–6916.

[15] M. Goor, S. Menkin, E. Peled, High power direct methanol fuel cell for mobility and portable applications, International Journal of Hydrogen Energy 44 (2018) 3138–3143.

[16] A. Afif, N. Radenahmad, Q. Cheok, S. Shams, J. H. Kim, A. K. Azad, Ammonia-fed fuel cells: A comprehensive review, Renewable and Sustainable Energy Reviews 60 (2016) 822–835.

[17] F. Abraham, I. Dincer, Thermodynamic analysis of Direct Urea Solid Oxide Fuel Cell in combined heat and power applications, Journal of Power Sources 299 (2015) 544–556.

[18] N. Radenahmad, A. Afif, P. I. Petra, S. M. Rahman, S. G. Eriksson, A. K. Azad, Proton-conducting electrolytes for direct methanol and direct urea fuel cells - A state-of-the-art review, Renewable and Sustainable Energy Reviews 57 (2016) 1347–1358.

[19] E. T. Sayed, T. Eisa, H. O. Mohamed, M. A. Abdelkareem, A. Allagui, H. Alawadhi, K.-j. Chae, Direct urea fuel cells : Challenges and opportunities, Journal of Power Sources 417 (2019) 159–175.

[20] S. Schemme, R. C. Samsun, R. Peters, D. Stolten, Power-to-fuel as a key to sustainable transport systems An analysis of diesel fuels produced from CO2 and renewable electricity, Fuel 205 (2017) 198–221.

[21] R. Lan, J. T. S. Irvine, S. Tao, Ammonia and related chemicals as potential indirect hydrogen storage materials, International Journal of Hydrogen Energy 37 (2012) 1482–1494.

[22] O. Elishav, D. R. Lewin, G. E. Shter, G. S. Grader, The nitrogen economy: Economic feasibility analysis of nitrogen-based fuels as energy carriers, Applied Energy 185 (2017) 183–188.

[23] M. Matzen, Y. Demirel, Technoeconomics and sustainability of renewable methanol and ammonia productions using wind power-based hydrogen, Journal of Advanced Chemical Engineering (2015).

[24] M. Matzen, Y. Demirel, Methanol and dimethyl ether from renewable hydrogen and carbon dioxide: Alternative fuels production and life-cycle assessment, Journal of Cleaner Production 139 (2016) 1068–1077.

[25] G. Dana, O. Elishav, A. Bardow, G. E. Shter, G. S. Grader, Nitrogen-Based Fuels:A Power-to-Fuel-to-Power Analysis, Angewandte Chemie - International Edition 55 (2016) 8798–8805.

[26] A. Tremel, P. Wasserscheid, M. Baldauf, T. Hammer, Techno-economic analysis for the synthesis of liquid and gaseous fuels based on hydrogen production via electrolysis, in: International Journal of Hydrogen Energy.

[27] Y. Bicer, I. Dincer, Life cycle evaluation of hydrogen and other potential fuels for aircrafts, International Journal of Hydrogen Energy 42 (2017) 10722–10738.

[28] D. Frattini, G. Cinti, G. Bidini, U. Desideri, R. Cioffi, E. Jannelli, A system approach in energy evaluation of different renewable energies sources integration in ammonia production plants, Renewable Energy 99 (2016) 472–482.

[29] G. Cinti, D. Frattini, E. Jannelli, U. Desideri, G. Bidini, Coupling Solid Oxide Electrolyser (SOE) and ammonia production plant, Applied Energy 192 (2017) 466–476.

[30] P. Baboo, M. Brouwer, J. Eijkenboom, M. Mohammadian, G. Notten, G. Prakash, The Comparison of Stamicarbon and Saipem Urea Tech-

nology Part 2 : The Materials and its failure modes, Technical Report, UreaKnowHow, 2016.

[31] S. Rönsch, J. Schneider, S. Matthischke, M. Schlüter, M. Götz, J. Lefebvre, P. Prabhakaran, S. Bajohr, Review on methanation - From fundamentals to current projects, Fuel 166 (2016) 276–296.

[32] M. A. Ancona, G. Antonioni, L. Branchini, A. De Pascale, F. Melino, V. Orlandini, V. Antonucci, M. Ferraro, Renewable Energy Storage System Based on a Power-to-Gas Conversion Process, Energy Procedia 101 (2016) 854–861.

[33] N. I. of Standard, Technology, Nist chemistry webbook, `https://webbook.nist.gov/chemistry/fluid/`, 2018. Last accessed on 13/03/2018.

[34] Y. Demirel, Energy. Production, Conversion, Storage, Conservation, and Coupling, Green Energy and Technology, Springer-Verlag London, 1 edition, 2012.

[35] G. Cinti, U. Desideri, SOFC fuelled with reformed urea, Applied Energy 154 (2015) 242–253.

[36] Power to Ammonia, Technical Report, Institute for Sustainable Process Technology, 2017.

[37] A. N. Rollinson, J. Jones, V. Dupont, M. V. Twigg, Urea as a hydrogen carrier: a perspective on its potential for safe, sustainable and long-term energy supply, Energy Environmental Science 4 (2011) 1216–1224.

[38] X. Su, J. Xu, B. Liang, H. Duan, B. Hou, Y. Huang, Catalytic carbon dioxide hydrogenation to methane: A review of recent studies, Journal of Energy Chemistry 25 (2016) 553–565.

[39] A. T. Portal, Audi e-gas, https://www.audi-technology-portal.de/en/mobility-for-the-future/audi-future-lab-mobility_en/audi-future-energies_en/audi-e-gas_en, 2013.

[40] M. Intitute, The methanol industry, http://www.methanol.org/the-methanol-industry/, 2018.

[41] J. Ott, V. Gronemann, F. Pontzen, E. Fiedler, G. Grossman, D. B. Kersebohm, G. Weiss, C. Witte, Ullmann's Encyclopedia of Industrial Chemistry-Methanol, Wiley-VCH Verlag GmbH & Co. KGaA, 2005.

[42] R. Rivera-Tinoco, M. Farran, C. Bouallou, F. Auprêtre, S. Valentin, P. Millet, J. R. Ngameni, Investigation of power-to-methanol processes coupling electrolytic hydrogen production and catalytic CO2 reduction, International Journal of Hydrogen Energy 41 (2016) 4546–4559.

[43] D. S. Kourkoumpas, E. Papadimou, K. Atsonios, S. Karellas, P. Grammelis, E. Kakaras, Implementation of the Power to Methanol concept by using CO2 from lignite power plants: Techno-economic investigation, International Journal of Hydrogen Energy 41 (2016) 16674–16687.

[44] K. Atsonios, K. D. Panopoulos, E. Kakaras, Investigation of technical and economic aspects for methanol production through CO2 hydrogenation, International Journal of Hydrogen Energy 41 (2016) 2202–2214.

[45] K. Atsonios, K. D. Panopoulos, E. Kakaras, Thermocatalytic CO2 hydrogenation for methanol and ethanol production: Process improvements, International Journal of Hydrogen Energy 41 (2016) 792–806.

[46] P. Esmaili, I. Dincer, G. F. Naterer, Development and analysis of an integrated photovoltaic system for hydrogen and methanol production, International Journal of Hydrogen Energy 40 (2014) 11140–11153.

[47] M. Chemicals, Mitsui chemicals, https://www.mitsuichem.com/index.htm, Last accessed on 13/03/2018.

[48] C. R. International, Resource efficiency by carbon recycling, http://carbonrecycling.is/, Last accessed on 13/03/2018.

[49] S. Frigo, R. Gentili, Analysis of the behaviour of a 4-stroke Si engine fuelled with ammonia and hydrogen, International Journal of Hydrogen Energy 38 (2013) 1607–1615.

[50] Urea-Based Fuel Cells and Electrocatalysts for Urea Oxidation, Energy Technology 4 (2016) 1329–1337.

[51] F. Guo, D. Cao, M. Du, K. Ye, G. Wang, W. Zhang, Y. Gao, K. Cheng, Enhancement of direct urea-hydrogen peroxide fuel cell performance by three-dimensional porous nickel-cobalt anode, Journal of Power Sources 307 (2016) 697–704.

[52] E. E. Agency, Co2 emission intensity table, https://www.eea.europa.eu/data-and-maps/daviz/co2-emission-intensity-3/download.table, Last accessed on 20/09/2018.

[53] U. D. o. E. Office of energy efficiency renewable energy, Doe technical targets for hydrogen production from electrolysis, https://www.energy.gov/eere/fuelcells/doe-technical-targets-hydrogen-production-electrolysis#distributed, Last accessed on 13/05/2019.

[54] I. Renewable, E. Agency, HYDROGEN FROM RENEWABLE POWER, September, 2018.

[55] P. Z. Ramchandra Bhandari, Clemens A. Trudewind, Life cycle assessment of hydrogen production via electrolysis e a review, Journal of Cleaner Production 85 (2014) 151–163.

[56] Italian Greenhouse Gas Inventory 1990-2013, National Inventory Report 2015, Technical Report, Istituto Superiore per la Protezione e la Ricerca Ambientale, 2015.